Scientific Research

Computer Generated Quadratic and Higher Order Apertures and Its Application on Numerical Speckle Images

Abdallah Mohamed Hamed

Physics Department, Faculty of Science, Ain Shams University, Cairo, Egypt
E-mail: *Amhamed*73@hotmail.com

Abstract

A computer generated quadratic and higher order apertures are constructed and the corresponding numerical speckle images are obtained. Secondly, the numerical images of the autocorrelation intensity of the randomly distributed object modulated by the apertures and the corresponding profiles are obtained. Finally, the point spread function (PSF) is computed for the described modulated apertures in order to improve the resolution.

1. Introduction

The modulated apertures were first suggested by the authors [1-5]. These apertures were proposed in order to improve the microscope resolution, in particular the coherent scanning optical microscopes (CSOM) [6-10].

The intensity pattern of speckle images may be considered as a superposition of the aperture spread function of an optical system and the classical speckle pattern [11,12]. The contrast may be affected by the PSF and it may be understood by considering the far—field speckle produced by weak diffuser [13].

Electronic/Digital speckle pattern interferometer (ESPI/DSPI) is a promising field that having a variety of applications [14-17], for example in the measurement of displacement/deformation, vibration analysis, contouring, non-destructive testing etc. The capability of ESPI/DSPI in displaying correlation fringes on a TV monitor is one of its distinct features. The digital speckle interferometer [18] (DSI) has many advantages since it does not need the photographic film and the optical dark room which are necessary for the holographic interferometers and the speckle photographs. The DSI has been used to the study of the density field in an acoustical wave for quantitative diagnosis of the speckle intensity. Digital data treatment is based on the direct computer aided correlation analysis of the temporal evolution of dynamic speckle pattern [19]. The evaluation procedure uses the autocorrelation analysis of the speckle pattern obtained with FFT and low pass noise filtering to check the statistical function of speckle intensity distribution.

In this paper, the numerical quadratic and higher order apertures are considered as a replacer of the thin film techniques. These apertures are placed nearly in the same plane of the randomly distributed object and the numerical speckle images are obtained. The difference between any two speckle images, for these different apertures, can be visualized by the human eye. Also, the autocorrelation intensity of the diffuser and the profile shapes are plotted. The autocorrelation intensity leads to the recognition of the aperture distribution in particular in case of the deformed aperture [12].

2. Theoretical Analysis

An aperture of ρ^n distribution is represented as follows:

$$P_n(\rho) = \rho^n \quad \text{with} \quad \left| \frac{\rho}{\rho_0} \right| \leq 1 \qquad (1)$$

$$= \text{zero} \quad \text{otherwise}$$

With $\rho = \sqrt{x^2 + y^2}$ is the radial coordinate in the aperture plane. This radial aperture is constructed, using MATLAB program, and is represented as shown in **Figure 1**, where $n = 2, 4, 6, \cdots, \text{etc}$. The point spread function (PSF) or the amplitude impulse response is calculated by operating the two dimensional Fourier transform to get $h_n(r)$ as follows [3,20]:

$$h_n(r) = \int_0^{\rho_0} \int_0^{2\pi} \rho^n \exp\left(-j2\pi \frac{\rho r}{\lambda f} \cos\theta \right) \rho \, \mathrm{d}\rho \, \mathrm{d}\theta$$

With the help of recurrence relations and using integration by parts [21], we get:

$$h_n(w) = const. \left\{ \frac{J_1(w)}{w} - \frac{nJ_2(w)}{w^2} + n(n-2)\frac{J_3(w)}{w^3} - \cdots \right\} \quad (2)$$

Where J_1 is the Bessel function of 1st order, and $r = \sqrt{u^2 + v^2}$ is the radial coordinate in the speckle plane and $w = \dfrac{2\pi\rho r}{\lambda f}$ is the reduced coordinate.

The rough surface used as a randomly distributed object may be considered as a statistical variation of the random component in surface height relative to a certain reference surface. Therefore, the random object used in this study is represented as follows:

$$\text{d}(x,y) = \exp[j\phi(x,y)] = \exp[2\pi j \, rand(N,N)] \quad (3)$$

$$j = \sqrt{-1}$$

A matrix of dimensions $N \times N = 1024 \times 1024$ pixels is considered to represent the diffuser or the randomly distributed object of height variations depend on the randomness of the function $rand(N,N)$ Equation (3). The height variation extends over the random range from zero up to maximum height equals unity.

The randomly distributed object $d(x,y)$ is a matrix of dimensions 1024×1024 is placed nearly in contact with the radial distributed ρ^n aperture $P_n(x,y)$ Hence, for coherent illumination like that emitted from laser beam, the transmitted amplitude is written as follows:

$$A(x,y) = \text{d}(x,y) . P_n(x,y) \quad (4)$$

The complex amplitude located in the focal plane of the lens L is obtained by operating the Fourier transform upon the complex amplitude $A(x,y)$, Equation (4), to get:

$$B(u,v) = F.T.\{A(X,Y)\} = F.T.\{\text{d}(x,y) . P_n(x,y)\} \quad (5)$$

Where F.T. refers to Fourier transform operation.

Making use of the properties of convolution product, Equation (5) becomes:

$$B(u,v) = F.T.\{\text{d}(x,y)\} * F.T.\{P_n(x,y)\} \quad (5)$$

$$B(u,v) = s(u,v) * h_n(u,v) \quad (6)$$

Where $s(u,v)$ is complex amplitude of speckle pattern formed in the focal plane of the lens L and is given by: $s(u,v) = F.T.\{\text{d}(x,y)\}$, while $h(u,v)$ is amplitude impulse response of the imaging system and is calculated by operating the Fourier transform upon the modulated aperture and is given by:

$$h_n(u,v) = F.T.\{P_n(x,y)\} .$$

The recorded intensity of the speckle image in the Fourier plane (u,v) is given by :

$$I(u,v) = |s(u,v) * h_{\text{modul}}(u,v)|^2 \quad (7)$$

The symbol $(*)$ stands for convolution operation.

This symbolic Equation (7) is explicitly written in integral form as follows:

$$I(u,v) = \left| \int\int_{-\infty}^{+\infty} s(u-u',v-v') * h_{\text{modul}}(u',v') \text{d}u' \text{d}v' \right|^2 \quad (8)$$

The difference between any two speckle images for two different modulated apertures of the same numerical aperture is obtained by subtraction, using formula (8), as follows :

$$\delta I = I_1 - I_2 \quad (9)$$

Where I_1 stands for the 1st speckle image and I_2 stands for the 2nd image.

We can reconstruct either of the diffuser image multiplied by the modulated aperture or the autocorrelation function of the diffuser.

Firstly, in order to reconstruct the diffuser which is modulated by the aperture it is sufficient to operate the inverse Fourier transform upon Equation (6), to get:

$$A(x',y') = F.T^{-1}\{B(u,v)\} \quad (10)$$

(x',y') is the imaging or reconstruction plane.

Substitute from Equation (6) in Equation (10), we get the diffuser function multiplied by the modulated aperture since the Fourier transform of the convolution product is transformed into multiplication [21,22]. Hence, we get in the Fourier plane (x',y'):

$$A(x',y') = \text{d}(x',y') . P(x',y') \quad (11)$$

Secondly, in order to reconstruct the autocorrelation function of the diffuser which is affected by the modulated radial aperture we are obliged to operate the Fourier transform upon the intensity distribution of the speckle pattern Equation (7), to get :

$$A_{auto}(x',y') = F.T.\{I(u,v)\} = F.T.\left\{|s(u,v) * h_{\text{modul}}(u,v)|^2\right\}$$

$$A_{auto}(x',y') = \{\text{d}(x',y').P_{\text{mod}}(x',y')\} * \{\text{d}(x',y').P_{\text{mod}}(x',y')\}^* \quad (12)$$

$$I(x',y') = |A_{auto}(x',y')|^2$$

Special case: If the impulse response of the imaging system is approximated by Dirac-Delta distribution *i.e.* $h_{\text{modul}}(u,v) = h(u,v) = \delta(u,v)$ which is valid only for uniform illumination like that obtained from laser beam by spatial filtering, then the speckle image becomes exactly the Fourier transform of the diffuser function as an object. Hence, Equation (7) becomes:

$$I(u,v) = |s(u,v) * \delta(u,v)|^2 = |s(u,v)|^2 \quad (13)$$

In this case, the reconstructed autocorrelation function of the diffuser is exactly the Fourier transform inverse of Equation (13):

$$A_{auto}(x',y') = \mathrm{d}(x',y') * \mathrm{d}^*(x',y') \qquad (14)$$

And the autocorrelation intensity is computed as the modulus square of Equation (14):

$$I(x',y') = |A_{auto}(x',y')|^2 \qquad (15)$$

3. Results and Discussion

A MATLAB program is constructed to design two selected radial apertures of quadratic ρ^2, and ρ^{10} distributions. These digital apertures are plotted as in **Figure 1 (a)** and **(b)** and compared with the uniform circular aperture and the linearly varied aperture [11].

Another MATLAB program is constructed to fabricate a diffuser as a randomly distributed object of dimensions 1024×1024 pixels shown in **Figure 2**.

The parts of MATLAB program are used to obtain the different **Figures (3)-(7)**. Digital speckle images for the randomly distributed objects which is modulated by the different apertures, using Equation (6), are represented in the **Figure 3**. The **Figure 3(a)** is plotted for the speckle image which is modulated by the linear aperture, the **Figure 3(b)** shows the speckle image modulated by the quadratic aperture, and the **Figure 3(c)** is given for higher order aperture ρ^{10}. It is shown, for the naked eye, that the three speckle images are different since they are modulated by different distributions of impulse responses or point spread function (PSF) shown in **Figures 9**. Also, the comparative speckle image, shown in **Figure 3(d)**, obtained for circular aperture is completely different from those speckle images shown in **Figure 3(a), (b) and (c)**.

If the difference between the modulated speckle images is not obvious for the naked eye, hence the computation of the difference between any two different modulated speckle images is recommended. **Figure 4(a), (b)** and **(c)** is showing the difference beference between the two speckle images correspondintween images. The difg to circular and quadratic apertures is plotted as in **Figure 4(a)** and the difference corresponding to the linear and quadratic apertures is plotted as in **Figure 4(b)** while the difference corresponding to the quadratic and higher order apertures of ϱ^{10} is shown in **Figure 4(c)**. These images which represent the difference between speckle images shown in **Figure 4(a), (b)** and **(c)** are clearly different since they are modulated by different apertures.

The profile shapes of the speckle patterns at slice $x = [1,256,128,128]$ and slice $y = [1,256,128,128]$ are plotted as shown in **Figures 5(a), (b)** and **(c)** and compared with

the profile corresponding to uniform circular aperture **Figure 5(d)** showing a great difference .

It is clear that the profile of the speckle image has a resolution which is dependent upon the aperture distribution. It is shown that resolution improvement is obtained for modulated speckle images, in particular in case of radial distributed apertures. This is attributed due to the improvement occurred in the point spread function of the imaging system. A comparison of the different PSF in case of circular, annular apertures, and radial distributed apertures is given later in **Figure 10(d)**. The reconstructed images of the apertures are obtained from Equation (11) and plotted in **Figures 6(a)** and **(b)**and the corresponding profiles are plotted as in **Figures 7(a), (b)** and **(c)**.

The difference between the actual analog image and the quantized digital image is called the quantization error. This quantization error may be minimized if the sampling rate is at least as great as the total spectral width w. Thus the critical sampling rate is just w called the Nyquist rate and the critical sampling interval is w^{-1} which is called the Nyquist interval.

The autocorrelation intensity of the diffuser, in case of modulated apertures Equation (12), is plotted as shown in **Figures 8(a), (b)** and **(c)**. It is shown, from these images, that the diameter of the autocorrelation intensity is twice the diameter of the whole circular aperture. Also, the contrast of the autocorrelation intensity is improved for the radial apertures as compared with the correlation images obtained in case of uniform apertures. The profiles of the autocorrelation intensity are plotted as in **Figures 9(a), (b)** and **(c)** which are taken at the slice $x = [1,256,128,128]$, and the slice $y = [1,256,128,128]$. It is shown that two different profiles are obtained for the two different apertures of ρ^2 and ρ^{10} distributions.

The point spread function is computed for apertures of ρ^n distribution using Equation (2) for different powers of even values of n. we take $n = 2, 4, 6, 8$, and 10. The PSF is represented graphically as shown in **Figure 10(a)** and **(b)**. The comparative curves corresponding to circular and annular apertures are plotted as in **Figure 10(c)**. It is shown, referring to the plotted results, that the best resolution is attained as n increases ($n = 10$) followed by n = 8 etc. Hence, the lowest resolution corresponds to the circular aperture and the best resolution corresponds to higher order aperture of $n = 10$ while the contrast of the image obtained in case of circular aperture is better than that obtained in case of higher order aperture. The **Figure 10(d)** shows three curves where the best resolution is attained for annular aperture at the expense of the contrast while the higher order aperture of ρ^{10} distribution gives better resolution and contrast as compared with circular aperture.
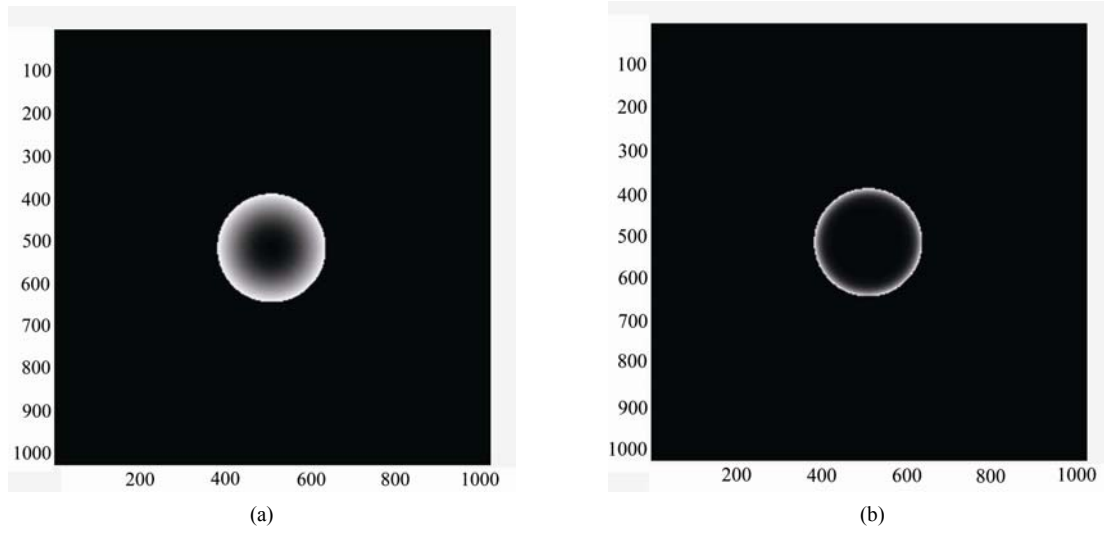
Figure 1. (a) The computer generated aperture having quadratic variations ρ^2 of dimensions 1024×1024; (b) The computer generated aperture having quadratic variations ρ^{10} of dimensions 1024×1024.
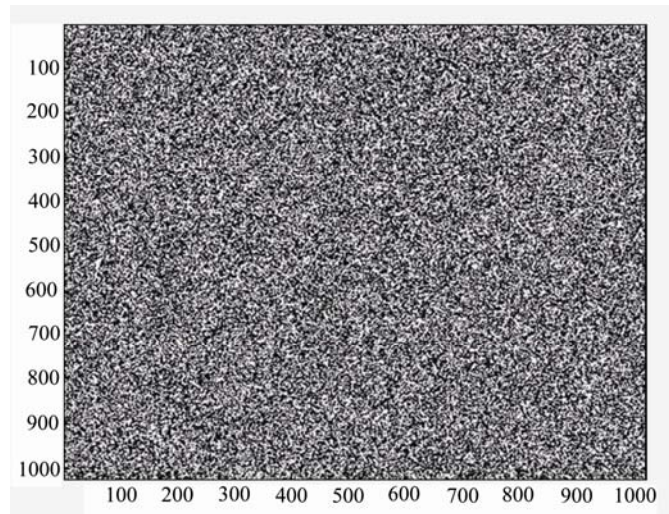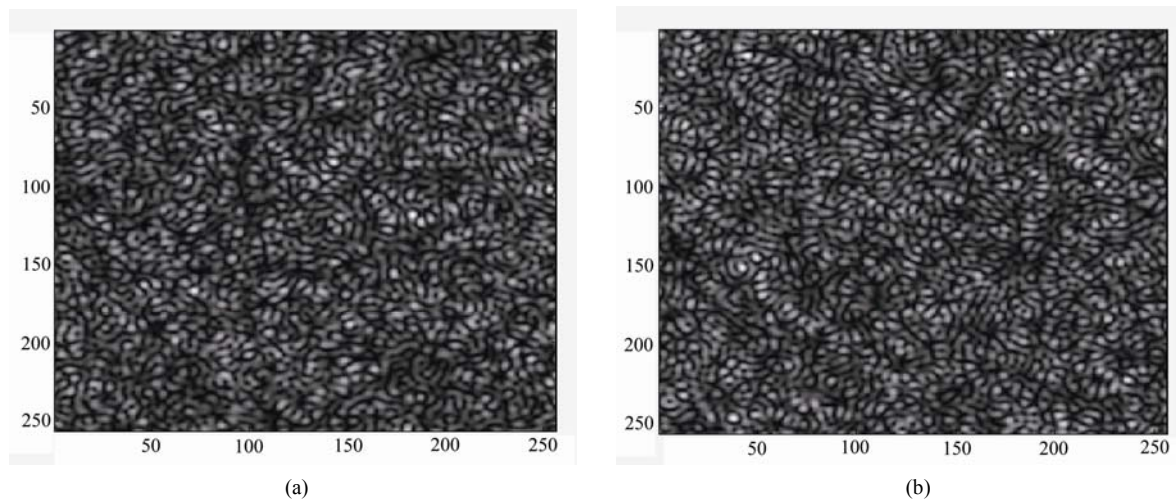

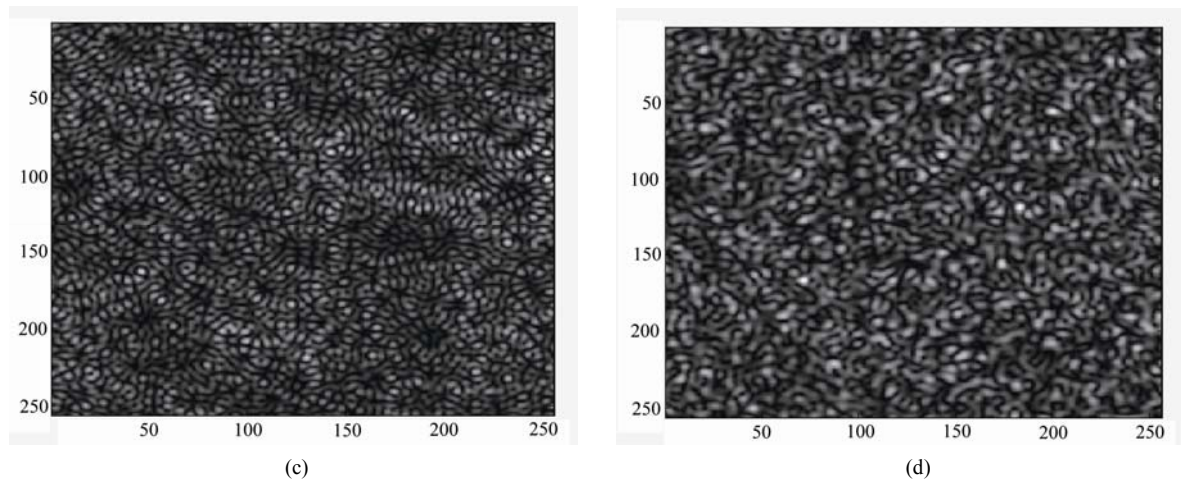**Figure 2. The randomly distributed object behave as a diffuser constructed numerically of dimensions 1024×1024.**

(a)   (b)

OPJ

(c)

(d)

Figure 3. (a) The numerical speckle image of the diffuser obtained in case of a linearly distributed aperture; (b) The numerical speckle image of the diffuser obtained in case of ρ^2 quadratic distributed aperture; (c) The numerical speckle image of the diffuser obtained in case of ρ^{10} distributed aperture; (d) Speckle image of randomly distributed object of dimensions 1024 × 1024 pixels using circular uniform aperture.
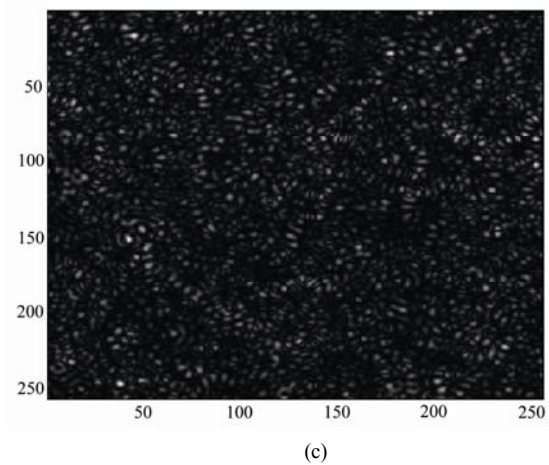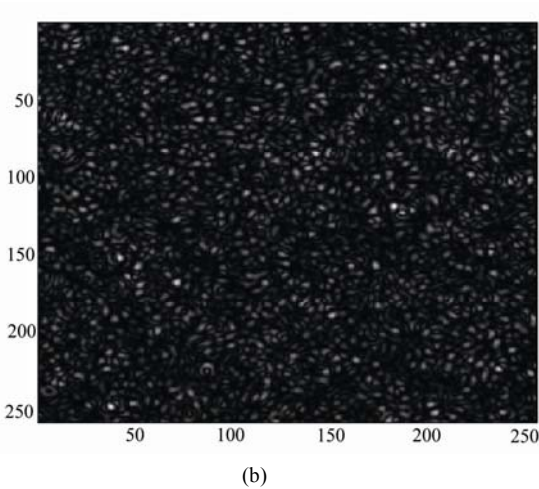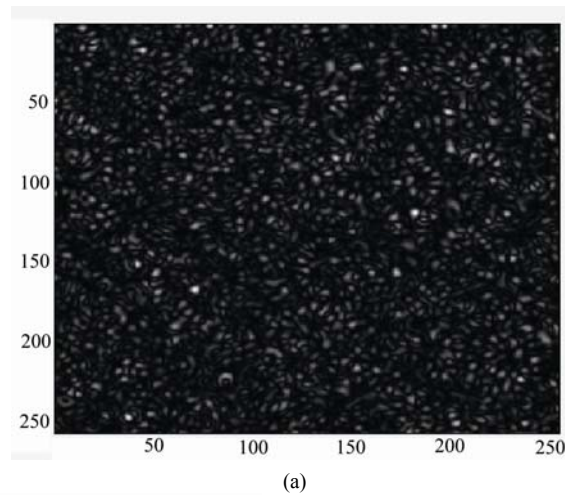

(a)

(b)

(c)

Figure 4. (a) The difference between the two speckle images corresponding to circular and quadratic apertures; (b) The difference between the two speckle images corresponding to the linear and quadratic apertures; (c) The difference between the two speckle images corresponding to the quadratic and higher order apertures of ϱ^{10}.
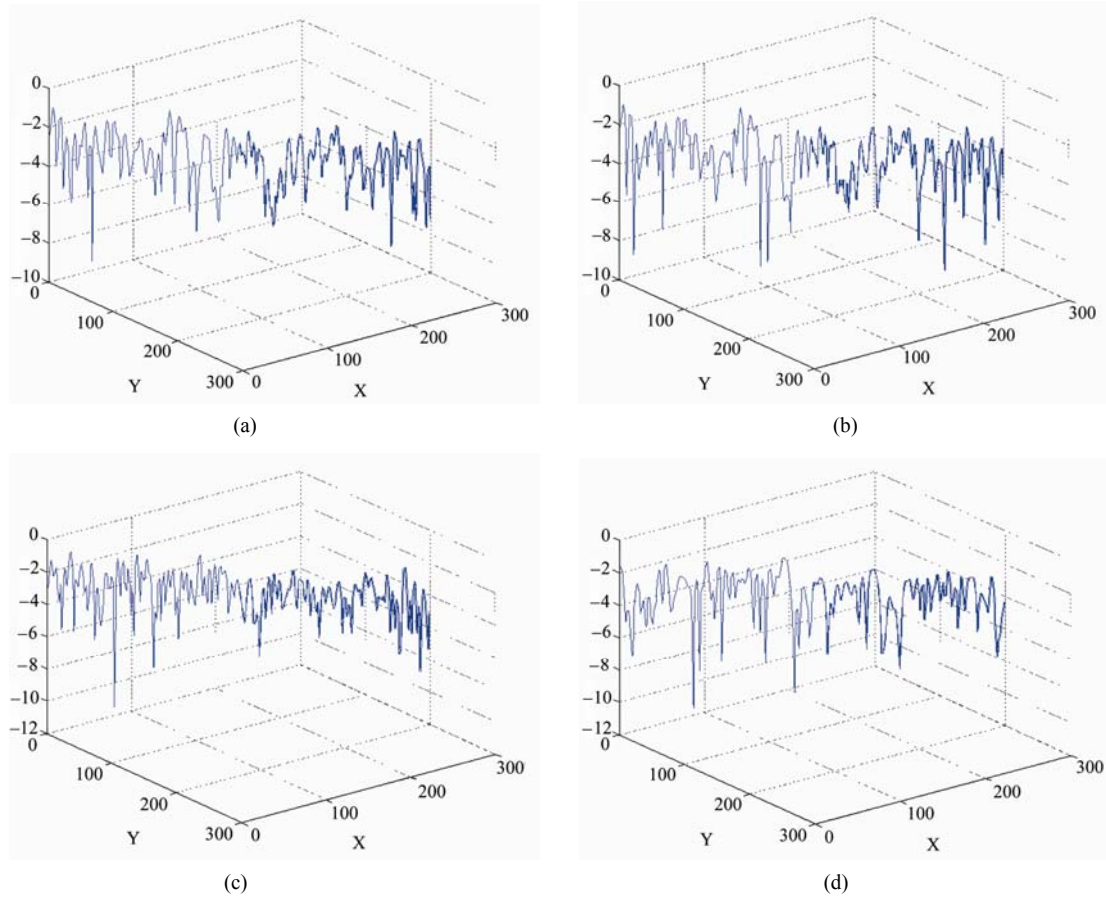
Figure 5. (a) The profile shape of the numerical speckle mage obtained using the linearly distributed aperture; (b) The profile shape of the numerical speckle image obtained using the quadratic aperture; (c) The profile shape of the numerical speckle image obtained in case of ρ^{10} distributed aperture; (d) The profile shape of the numerical speckle image obtained in case of uniform circular aperture.
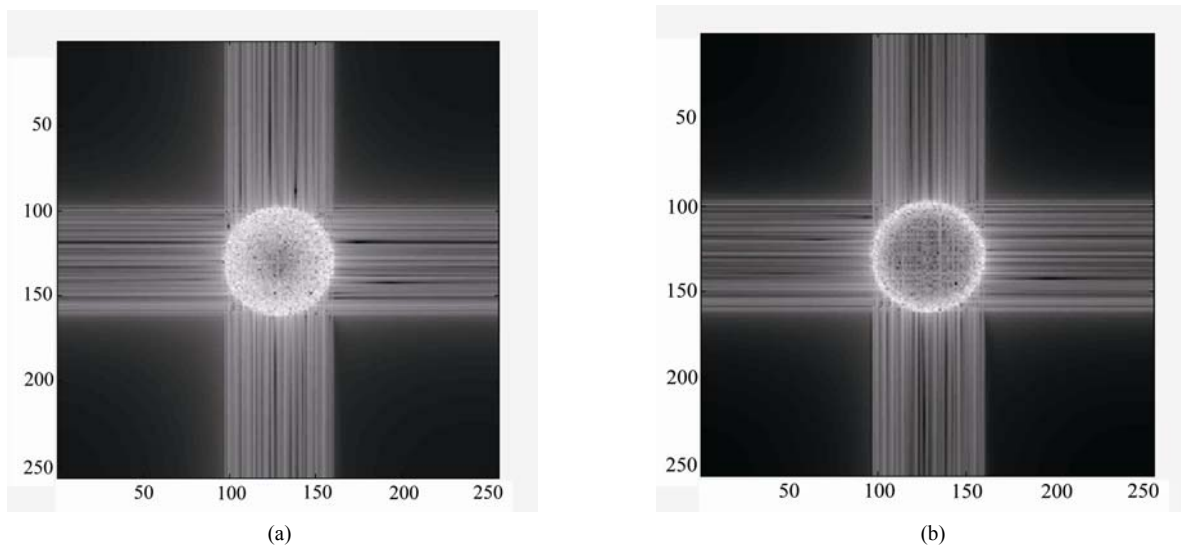

Figure 6. (a) Reconstruction of the quadratic aperture obtained from the modulated speckle image shown in Figure 3(b); (b) Reconstruction of the ρ^{10} aperture obtained from the modulated speckle image shown in Figure 3(c).

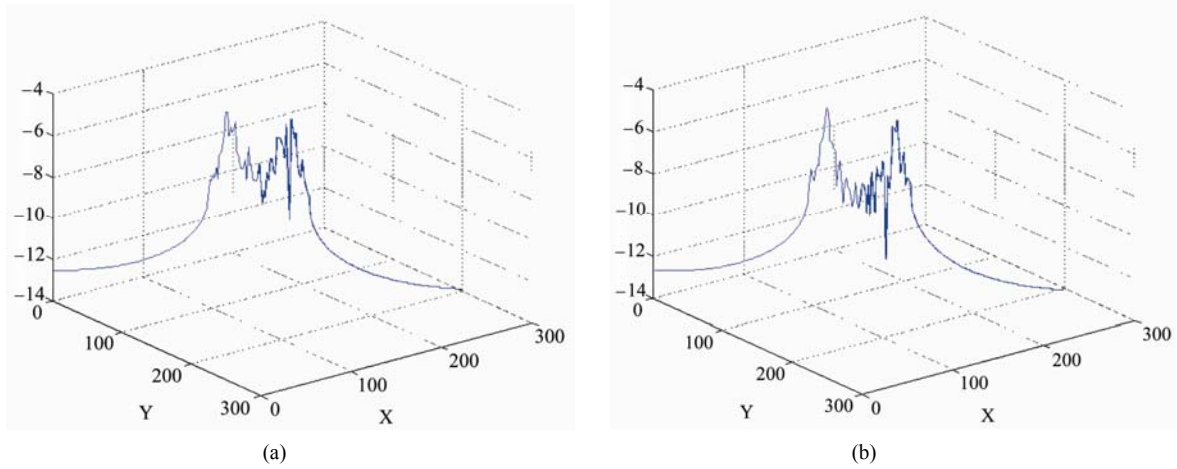(a)   (b)

Figure 7. (a) Profile shape of the reconstructed quadratic aperture; (b) Profile shape of the reconstructed ρ^{10} aperture.

(a)   (b)
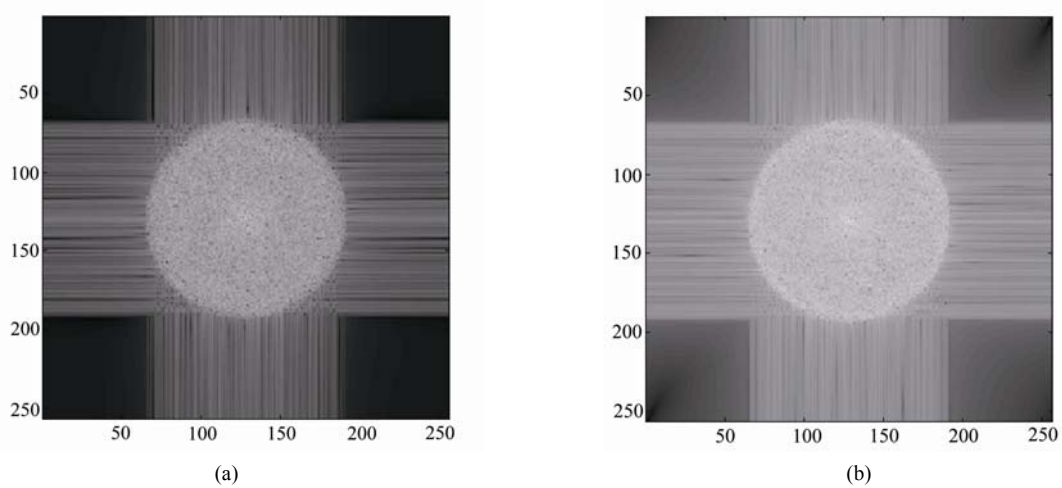
Figure 8. (a) The numerical image of the autocorrelation intensity of the diffuser modulated by the quadratic ρ^2 aperture; (b) The numerical image of the autocorrelation intensity of the diffuser modulated by ρ^{10} distributed aperture.

(a)   (b)
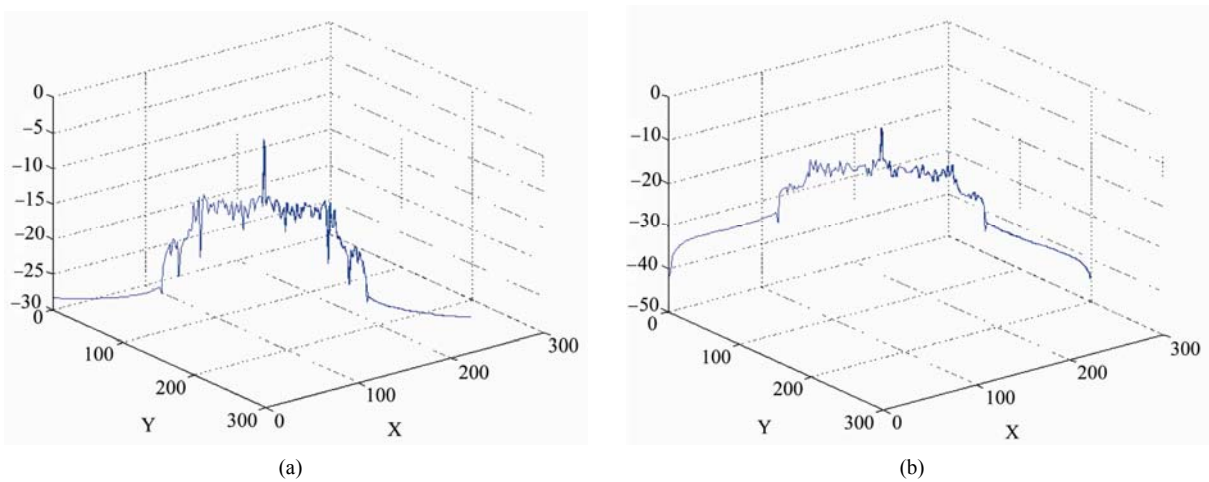
Figure 9. (a) The profile of the autocorrelation intensity obtained from Figure 8(a) Slice x = [1,256,128,128] and Slice y = [1 256,128,128]; (b) The profile of the autocorrelation intensity obtained from Figure 8(b) Slice x = [1,256,128,128] and Slice y = [1,256,128,128].
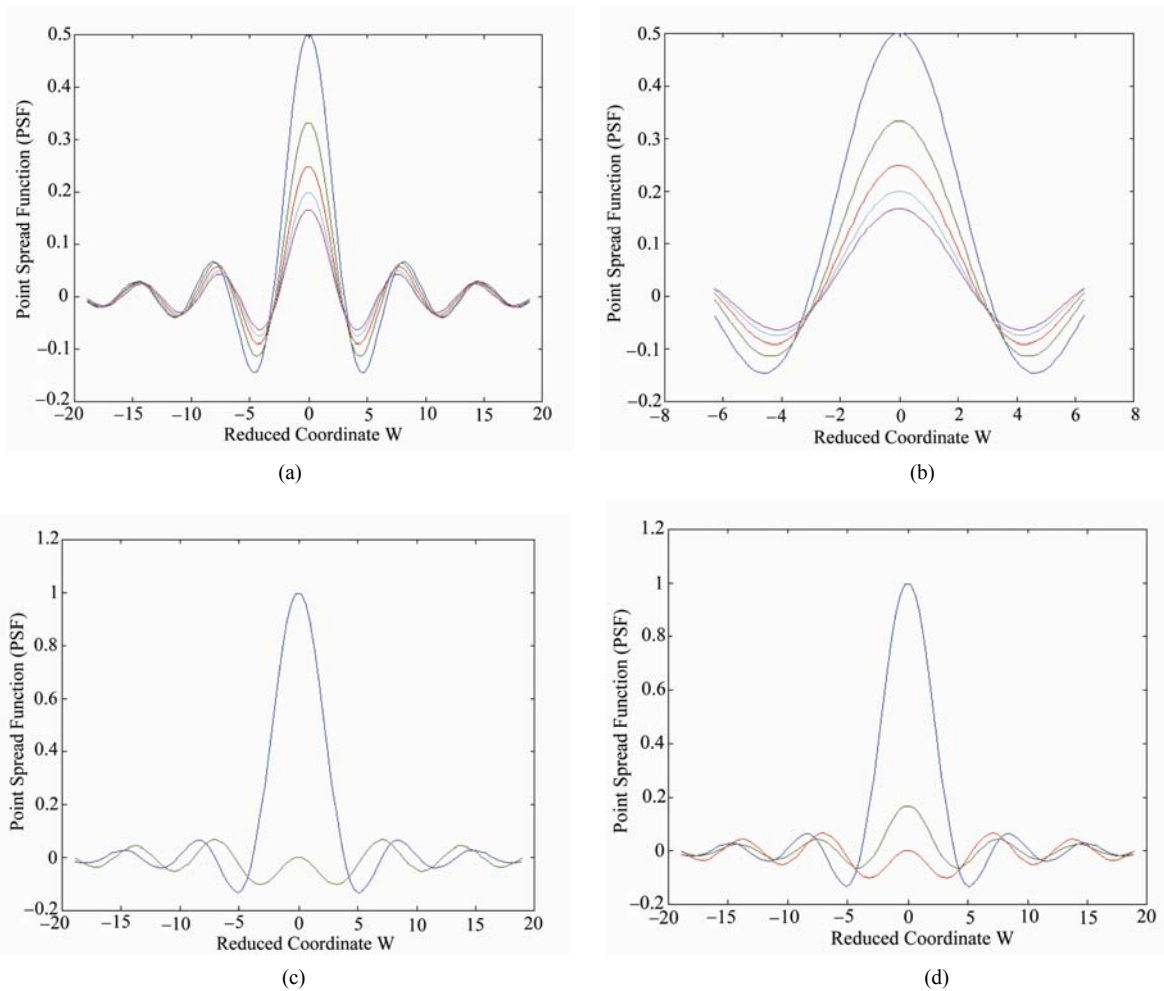
Figure 10. (a) The plot of the point spread function (PSF) corresponding to five different apertures. The highest blue curve is plotted for the quadratic aperture of *n* = 2 .The green curve corresponds to *n* = 4, the red for *n* = 6, the lowers are plotted for *n* = 8 , and *n* = 10. The range of w equals [–6, 6]; (b) The same plot shown in Figure 9 but in the range of w extends from [–2,2] for the sake of clarity and comparison. The resolution is improved by increasing the order *n* quadratically; (c) Two curves are plotted for the PSF where the highest curve is plotted for the circular aperture while the lowest is for the annular aperture of width 0.1. where is the radius of the circular aperture; (d) Three curves are plotted for the PSF where the highest curve is Plotted for the circular aperture while the lowest is for the annular aperture of width 0.1. Where ρ is the radius of the circular aperture and the intermediate green curve corresponds to higher order aperture of *n* = 10.

4. Conclusions

We have computed numerically the autocorrelation intensity of the randomly distributed object, using three different apertures, from the speckle images. It is concluded that, from the shape of the autocorrelation intensity for both of the modulated apertures, the diameter of the autocorrelation peak is two times the diameter of the whole aperture as expected. Also, the contrast of the modulated speckle images is affected by the modulated apertures. It is shown that the contrast for quadratic aperture is better than the contrast obtained in case of higher order aperture.

The radial higher order PSF curve is better in resolu-

tion than for the circular aperture since the central peak of the PSF for higher order aperture is sharper than the corresponding peak obtained for the circular aperture. The contrast is better for the circular aperture since it depends mainly on the numerical aperture without modulation.

The PSF plot for higher order apertures of ρ^n distributions showed a great improvement in resolution as compared with that obtained in case of uniform circular aperture.

The potential application of the computerized modulated apertures on metrological systems, such as digital speckle interferometers and holographic filters, lies in its facility of fabrication as compared with the tedious work

necessary in thin film techniques.

5. References

[1] J. J. Clair and A. M. Hamed, "Theoretical Studies on Optical Coherent Microscope," *Optik*, Vol. 64, No. 2, 1983, pp. 133-141.

[2] A. M. Hamed and J. J. Clair, "Image and Super-Resolution in Optical Coherent Microscopes," *Optik*, Vol. 64 , No. 4, 1983, pp. 277-284.

[3] A. M. Hamed and J. J. Clair, "Studies on Optical Properties of Confocal Scanning Optical Microscope Using Pupils with Radial Transmission," *Optik*, Vol. 65, No. 3, 1983, pp. 209-218.

[4] A. M. Hamed, "Resolution and Contrast in Confocal Optical Scanning Microscopes," *Optics and Laser Technol*ogy, Vol. 16, No. 2, 1984, pp. 93-96. doi:10.1016/0030-3992(84)90061-6

[5] A. M. Hamed, "A Study on Amplitude Modulation and an Application on Confocal Imaging," *Optik*, Vol. 107 No. 4, 1998, pp. 161-164.

[6] T. Wilson, "Imaging Properties and Applications of Scanning Optical Microscopes," *Applied Physics*, Vol. 22, No. 2, 1980, pp. 119-128. doi:10.1007/BF00885994

[7] C. J. R. Sheppard and A. Choudhary, "Image Formation in the Scanning Microscope," *Journal of Modern Optics*, Vol. 24, No. 10, 1977, pp. 1051-1073.

[8] G. Nomarski, *The Journal of the Optical Society of America*. Vol. 65, No. 10, 1975, p. 1166.

[9] C. J. R. Sheppard and T. Wilson, "Image Formation In Scanning Microscopes with Partially Coherent Source and Detector," *Journal of Modern Optics*, Vol. 25, No. 4, 1978, pp. 315-325.

[10] I. J. Cox, C. J. R. Sheppard and T. Wilson, "Improvement in Resolution by Nearly Confocal Microscopy," *Applied Optics*, Vol. 21, No. 5, 1982, pp. 778-781. doi:10.1364/AO.21.000778

[11] A. M. Hamed, "Numerical Speckle Images Formed by Diffusers Using Modulated Conical and Linear Apertures," *Journal of Modern Optics*, Vol. 56, No. 10, 2009, pp. 1174-1181. doi:10.1080/09500340902985379

[12] A. M. Hamed, "Formation of Speckle Images Formed For Diffusers Illuminated by Modulated Aperture (Circular Obstruction)," *Journal of Modern Optics*, Vol. 56, No. 15, 2009, pp. 1633-1642. doi:10.1080/09500340903277792

[13] R. D. Bahuguna, "Speckle Patterns of Weak Diffusers: Effect of Spherical Aberration," *Applied Optics*, Vol. 19, No. 11, 1980, pp. 1874-1878. doi:10.1364/AO.19.001874

[14] H. El-Ghandoor and A. M. Hamed, "Strain Analysis Using TV Interferometer," *International Symposium on the Technologies for Optoelectronics Conference*, Cannes, Vol. 683, No. 30, 1987.

[15] G. A. Slettemoen, "General Analysis of Fringe Contrast in Electronic Speckle Pattern Interferometer," *Optica Acta*, Vol. 26, No. 3, 1979, pp. 313-327.

[16] G. A. Slettemoen, "Optimal Signal Processing in Electronic Speckle Pattern Interferometer (ESPI)," *Optics Communications*, Vol. 23, No. 2, 1977, pp. 213-216. doi:10.1016/0030-4018(77)90309-1

[17] R. S. Sirohi and A. R. Ganesan, "Holographic Systems, Components and Applications," *Proceedings of the 2nd International Conference on IEEE*, 1989.

[18] Y. Z. Song and H. L. Zhang, etc., "Dynamic Digital Speckle Interferometry Applied to Optical Diagnosis of Gas-Liquid Phase Change," *The International Society for Optical Engineering*, Vol. 4448, 2009, pp. 111-119.

[19] C. Greated, E. Lavinskaya and N. Fomin, "Numerical Simulation of Acoustical Wave Tracing," *Journal of Mathematical Modelling*, *Russian Academy of Science*, Vol. 15, No. 7, 2003, pp. 75-80.

[20] J. W. Goodmann, "Introduction to Fourier Optics and Holography," McGraw-Hill book Company, New York, 1968.

[21] J. D. Gaskill, "Linear Systems, Fourier Transforms, and Optics," John Wiley &Sons, Inc., New York, 1978.